International Journal of Modern Physics E

New results from the Bates Large Acceptance Spectrometer Toroid (BLAST)

Haiyan Gao

Department of Physics and the Triangle Universities Nuclear Laboratory, Duke University, Durham, North Carolina 27708, U.S.A.
gao@phy.duke.edu

and the BLAST Collaboration

Received (received date)
Revised (revised date)

An experiment using the novel technique of scattering a longitudinally polarized electron beam from polarized internal hydrogen/deuterium gas targets was carried out in the South Hall Ring at the MIT-Bates Accelerator Center. The scattered particles were detected by the Bates Large Acceptance Spectrometer Toroid (BLAST) detector. The proton electric to magnetic form factor ratio, $\frac{G_E^p}{G_M^p}$ at Q^2= 0.1 - 0.65 $(\mathrm{GeV/c})^2$ has been determined from the experiment by measuring the spin-dependent ep elastic scattering asymmetry in the two symmetric sectors of the BLAST simultaneously for the first time. The neutron electric form factor G_E^n in the same Q^2 range has been extracted by measuring the spin-dependent asymmetry from the $\vec{d}(\vec{e}, e'n)$ process with a vector polarized deuterium target. These results on the nucleon form factors from the BLAST experiment are presented.

1. Introduction

The nucleon electromagnetic form factors are fundamental quantities related to the distribution of charge and magnetization within nucleons. While Quantum Chromodynamics (QCD) has been extremely well tested in the high energy regime, where perturbative QCD is applicable, understanding confinement and hadron structure in the non-perturbative region of QCD remains challenging.

The proton electric (G_E^p) and magnetic (G_M^p) form factors have been studied extensively in the past from unpolarized electron-proton (ep) elastic scattering using the Rosenbluth separation technique [1]. Recent advances in polarized beams, targets, and polarimetry have resulted in a new class of experiments extracting $\mu G_E^p/G_M^p$ from polarization measurements. Data from polarization transfer experiments at Jefferson Lab [2,3,4] measuring this ratio directly with unprecedented precision, show that $\frac{\mu G_E^p}{G_M^p}$ drops to approximately 0.3 at the highest measured and published Q^2 value ($\sim$ 5.5 $(\mathrm{GeV/c})^2$). This is very different from unity, as suggested by earlier unpolarized cross section measurements [5,6] and verified by recent experiments [7,8].

Such recoil polarization measurements have been extended to a Q^2 value of about 9 (GeV/c)^2 at Jefferson Lab [9].

These new data [2,3] suggest that the proton Dirac ($F_1(Q^2)$) and Pauli form factors ($F_2(Q^2)$) scale as $Q\frac{F_1}{F_2} \sim$ constant at large values of Q^2, instead of $Q^2\frac{F_1}{F_2} \sim$ constant, as suggested by the previous unpolarized data. The Q^2 scaling was believed to occur because contributions from nonzero parton orbital angular momentum were power suppressed, as shown by Lepage and Brodsky [10]. However, an explicit pQCD calculation [11] including these contributions shows an asymptotic scaling of the proton form factor ratio: $F_2(Q^2)/F_1(Q^2) \sim (\log^2 Q^2/\Lambda^2)/Q^2$ with 0.2 GeV$\leq \Lambda \leq$0.4 GeV. The $F_2(Q^2)/F_1(Q^2) \sim 1/\sqrt{Q^2}$ scaling behavior was obtained by Ralston [12] and Miller [13] using calculations involving parton orbital angular momentum. A nonperturbative analysis [14] of the hadronic form factors based on light-front wave functions was also carried out. All these approaches [11,12,13,14] describe the JLab proton form factor data [2,3,4] well.

While the intriguing Q^2 dependence of the proton form factor ratio can be described [11,12,13,14], it is important to understand the discrepancy between results obtained from recoil proton polarization measurements and those from the Rosenbluth method. New Jefferson Lab data [7] from Rosenbluth separations are in good agreement with previous SLAC results. Recently, a new "Super-Rosenbluth" experiment was carried out at Jefferson Lab [8], in which the struck protons were detected instead of the electron to minimize systematic uncertainties associated with the large variation of energy of the scattered electron. These new results agree with previous Rosenbluth experiments, suggesting some fundamental differences in the formalism of polarized and unpolarized extractions of the form factor ratio. Two-photon exchange contributions [15] are believed to contribute to the observed discrepancy between the polarization method and the Rosenbluth technique. Currently, there are intensive efforts in both theory [16] and experiment [17] aiming at understanding the two-photon exchange contributions to electron scattering in general, particularly with respect to the aforementioned discrepancy in the proton form factor ratio.

We recently completed a new experiment [21] in which longitudinally polarized electrons were scattered from a polarized proton target at the MIT-Bates accelerator Laboratory. The proton electric to magnetic form factor ratio can be extracted from the spin-dependent asymmetry with high precision up to a Q^2 value of about 0.6 (GeV/c)^2. Such a double-polarization experiment is important because it employs a completely different experimental technique with different systematic uncertainties than recoil proton polarization measurements. Although the Q^2 range of this experiment is quite low compared with Jefferson Lab recoil proton polarization experiments [2,3,4], this experiment paved the way for future polarized electron polarized target measurements at Jefferson Lab at much higher Q^2 values.

Measurements of the neutron electric form factor are extremely challenging because of the lack of free neutron targets, the smallness of G_E^n, and the dominance of the magnetic contribution to the unpolarized differential cross-section. A promis-

ing approach to measure G_E^n is by using polarization degrees of freedom. One can employ a polarized deuteron target and a longitudinally polarized electron beam to probe the neutron electric form factor by the $\vec{d}(\vec{e}, en)$ reaction. Recoil polarization measurements from $d(\vec{e}, e'\vec{n})$ have also been carried out by a number of experiments as well as polarization measurements from $^3\vec{H}e(\vec{e}, e'n)$ using polarized ^{3}He targets. Details on such measurements can be found in [22,23]. The BLAST experiment carried out measurements on the neutron electric form factor using the $\vec{d}(\vec{e}, en)$ reaction. Precision measurements of all nucleon form factors both at small and large values of Q^2 are important for our understanding of the nucleon structure as well as for testing the state-of-the-art calculation of the nucleon form factor.

The rest of the paper is organized as the following. In section II and III, we introduce the formalism for double polarized electron-proton scattering and polarized quasifree electron scattering from a vector polarized deuteron target. We then discuss the BLAST experiment followed by results on nucleon electromagnetic form factors.

2. Spin-dependent electron-proton elastic scattering

The spin-dependent asymmetry for elastic e-p scattering with longitudinally polarized electrons and a polarized proton target has the following form [24]:

$$A = \frac{\Delta}{\Sigma} = -\frac{2\tau v_{T'} \cos\theta^* {G_M^p}^2 - 2\sqrt{2\tau(1+\tau)} v_{TL'} \sin\theta^* \cos\phi^* G_M^p G_E^p}{(1+\tau) v_L {G_E^p}^2 + 2\tau v_T {G_M^p}^2} , \quad (1)$$

where θ^*, ϕ^* are the target spin polar and azimuthal angles defined relative to the three-momentum transfer vector of the virtual photon, and v_k are kinematic factors [24]. The experimental asymmetry A_{exp}, is related to the spin-dependent asymmetry of Eqn. 1 by the relation

$$A_{exp} = P_b P_t A , \quad (2)$$

where P_b and P_t are the beam and target polarizations, respectively. A determination of the ratio $\frac{G_E^p}{G_M^p}$, independent of the knowledge of the beam and target polarization, can be precisely obtained by forming the so-called super ratio [22]:

$$R = \frac{A_1}{A_2} = \frac{2\tau v_{T'} \cos\theta_1^* {G_M^p}^2 - 2\sqrt{2\tau(1+\tau)} v_{TL'} \sin\theta_1^* \cos\phi_1^* G_M^p G_E^p}{2\tau v_{T'} \cos\theta_2^* {G_M^p}^2 - 2\sqrt{2\tau(1+\tau)} v_{TL'} \sin\theta_2^* \cos\phi_2^* G_M^p G_E^p} , \quad (3)$$

where A_1 and A_2 are elastic electron-proton scattering asymmetries measured at the same Q^2 value, but two different proton spin orientations relative to the corresponding three-momentum transfer vector, i.e., (θ_1^*, ϕ_1^*) and (θ_2^*, ϕ_2^*), respectively.

For a detector configuration that is symmetric with respect to the incident electron momentum direction, A_1 and A_2 can be measured simultaneously by forming two independent asymmetries with respect to either the electron beam helicity or the target spin orientation in the beam-left and beam-right sector of the detector

system, respectively. The target spin direction would be chosen to optimize the determination of the proton form factor ratio given the experimental running conditions and the running time. In the BLAST experiment [21], the target spin angle was aligned at approximately 45° with respect to the beam line.

3. Polarized Quasielastic Electron-Deuteron Scattering and Neutron Electromagnetic Form Factors

The scattering cross-section for longitudinally polarized electrons from a polarized deuteron target for the $\vec{d}(\vec{e}, en)$ reaction can be written as [24,26]:

$$S = S_0 \left\{1 + P_1^d A_d^V + P_2^d A_d^T + h(A_e + P_1^d A_{ed}^V + P_2^d A_{ed}^T)\right\}, \tag{4}$$

where S_0 is the unpolarized differential cross section, h the polarization of the electrons, and P_1^d (P_2^d) the vector (tensor) polarization of the deuteron. A_e is the beam analyzing power, $A_d^{V/T}$ the vector and tensor analyzing powers, and $A_{ed}^{V/T}$ the vector and tensor spin-correlation parameters. The polarization direction of the deuteron is defined with respect to the three-momentum transfer vector, $\vec{q}$. The vector spin-correlation parameter A_{ed}^V contains a term representing the interference between the small neutron electric form factor and the dominant neutron magnetic form factor, when the target spin is perpendicular to the $\vec{q}$ vector direction. Thus, the spin-dependent asymmetry (defined with respect to the electron beam helicity) from the $\vec{d}(\vec{e}, en)$ reaction for vector polarized deuteron gives access to the quantity $\frac{G_E^n}{G_M^n}$ to first order when the target spin direction is aligned perpendicular to $\vec{q}$. Such experiments are extremely challenging since they involve both neutron detection and a vector polarized deuteron target.

The spin-dependent contribution to the inclusive $\vec{\mathrm{d}}(\vec{e}, e')$ cross section from a longitudinally polarized electron beam and a vector polarized deuteron target is completely contained in two spin-dependent nuclear response functions, a transverse response $R_{T'}$ and a longitudinal-transverse response $R_{TL'}$ [24]. These appear in addition to the spin-independent longitudinal and transverse responses R_L and R_T. These spin-dependent response functions $R_{T'}$ and $R_{TL'}$ can be isolated experimentally by forming the spin-dependent asymmetry A defined previously with respect to the electron beam helicity. In terms of the nuclear response functions, A can be written [24]:

$$A = \frac{-\cos\theta^* \nu_{T'} R_{T'} + 2\sin\theta^* \cos\phi^* \nu_{TL'} R_{TL'}}{\nu_L R_L + \nu_T R_T} \tag{5}$$

where the ν_k are kinematic factors, and θ^* and ϕ^* are the target spin angles defined previously. The response functions R_k depend on Q^2 and the electron energy transfer ω. By choosing $\theta^* = 0$, *i.e.* by orienting the target spin parallel to the momentum transfer $\vec{q}$, one selects the transverse asymmetry $A_{T'}$ (proportional to $R_{T'}$); by orienting the target spin perpendicular to the momentum transfer $\vec{q}$ ($\theta^* = 90$, $\phi^* = 0$), one selects the transverse-longitudinal asymmetry $A_{TL'}$ (proportional to $R_{TL'}$). $R_{T'}$ at quasi-elastic kinematics contains a dominant magnetic contribution

and is essentially proportional to $(G_M^n)^2 + (G_M^p)^2$. Therefore, one can determine the neutron magnetic form factor from the inclusive asymmetry measurement once the proton magnetic form factor has been determined.

4. The BLAST experiment

The BLAST experiment was designed to carry out spin-dependent electron scattering from hydrogen [21] and light nuclei. Details on the experimental setup can be found in Hasell *et al.* [27]. The experiment was carried out in the South Hall Ring of the MIT Bates Linear Accelerator Center, which stored an intense polarized beam with a beam current of 250 mA and longitudinal electron polarization around 65%. A Siberian Snake in the ring opposite of the interaction point preserved the electron polarization, which was continuously monitored with a Compton polarimeter installed upstream of the internal target region. The background was minimized with a tungsten collimator in front of the target cell.

The electrons scattered off polarized protons from an Atomic Beam Source (ABS) internal target, in a cylindrical target cell 60 cm long by 15 mm in diameter. The ABS provided a highly polarized ($P_t \sim 0.8$) isotopically pure target without windows in the beam line, and with fast spin reversal to reduce systematic errors. The ABS was operated in single state mode in order to avoid depolarization due to hyperfine interactions. The ABS switched between states every five minutes and the ring was filled with alternating electron polarizations every half hour. In the case of deuterium, the ABS produced polarized mono-atomic deuterium gas in the storage cell with nuclear vector ($V+$: m=1; $V-$: m=-1) and tensor ($T-$: m=0) polarization states. Details about the ABS can be found in Cheever *et al.* [28].

The relatively low luminosity $L = 1.6 \times 10^{31}\mathrm{cm}^{-2}\mathrm{s}^{-1}$ of the internal gas target was compensated by the large acceptance spectrometer. The symmetric detector package was built around eight copper coils which provided the 0.38 Tesla BLAST toroidal magnetic field. Two of the sectors were instrumented with three drift chambers for momentum, angle, and position determination, scintillators for triggering and time-of-flight, and Čerenkov detectors for pion rejection. Additional scintillators at backward angles beyond the drift chambers extended the acceptance to $Q^2 = 0.85(\mathrm{GeV/c})^2$. The neutron detectors were enhanced in the right sector with a detection efficiency of $\sim$ 30% as compared to $\sim$ 10% in the left sector due to the choice of the target spin angle. The setup allowed simultaneous measurements of the $\vec{d}(\vec{e}, e'p)$, $\vec{d}(\vec{e}, e'd)$ in addition to the $\vec{d}(\vec{e}, e')$ and the $\vec{d}(\vec{e}, e'n)$ processes. The schematics of the BLAST detector is shown in Fig. 1.

The elastic events for *ep* elastic scattering were selected with a cut on the invariant mass of the scattered electron, and a vertex cut, and fiducial cuts on the acceptance. These cuts were also consistent with kinematic cuts on the 3-momentum of the recoil proton, and timing and co-planarity cuts on the scintillators. These cuts were sufficient to reduce the background to less than 1%. The background was measured with 14.9 kC of integrated beam charge on the same target cell without

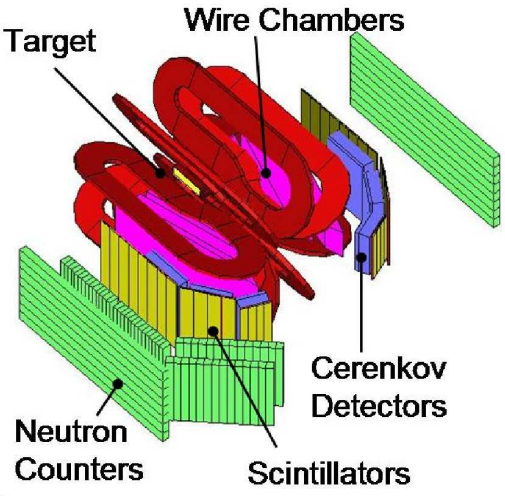

Fig. 1. A schematics of the BLAST detector setup.

hydrogen gas flowing in the target cell. The beam blowup effect was shown to be negligible by measuring the H(e,e′n) rates between hydrogen and the empty target. The first hydrogen production run in December 2003 accumulated 3.4 pb^{-1} of integrated luminosity with the target polarization $P_t = 0.48 \pm 0.04$ and the BLAST field reversed to access lower values of Q^2. The second run in April 2004 accumulated 9.6 pb^{-1} with $P_t = 0.42 \pm 0.04$ and the nominal BLAST field. Another 98 pb^{-1} have been accumulated in the third run completed in December 2004, with target polarization improved to $P_t = 0.80$. In our final analysis [21], a single value of $P_b P_t$ was fit for all Q^2 values for optimal extraction of the form factor ratio [25], resulting in $P_b P_t = 0.537 \pm 0.003$ (stat) $\pm$ 0.007 (sys).

The selection of $d(e, e'n)$ events is very clean and the number of proton tracks misidentified as neutrons is negligible, due to the highly efficient charged particle veto provided by the thin scintillator bars and the large-volume drift chambers in front of the neutron detectors. A set of cuts applied on the time correlation between the charged and the neutral track, and on kinematic constraints for the electrodisintegration process, was employed to identify the quasielastic $d(e, e'n)$ events. The background from scattering off the aluminum target cell walls, measured with a hydrogen (empty) target, is less than 4% (3%) of the normalized yield obtained with deuterium. There were two data collection periods for the deuterium running: 451 kC of accumulated charge in 2004 with the target spin angle of 32° and 503 kC in 2005 with a target spin angle of 47°. The average product of beam and target polarization determined from the $\vec{\mathrm{d}}(\vec{\mathrm{e}},\mathrm{e'p})$ reaction was $P_e P_z = 0.5796 \pm 0.0034(\mathrm{stat}) \pm 0.0034(\mathrm{sys})$ in the first and $0.5149 \pm 0.0043(\mathrm{stat}) \pm 0.0054(\mathrm{sys})$ in the second data set [29].

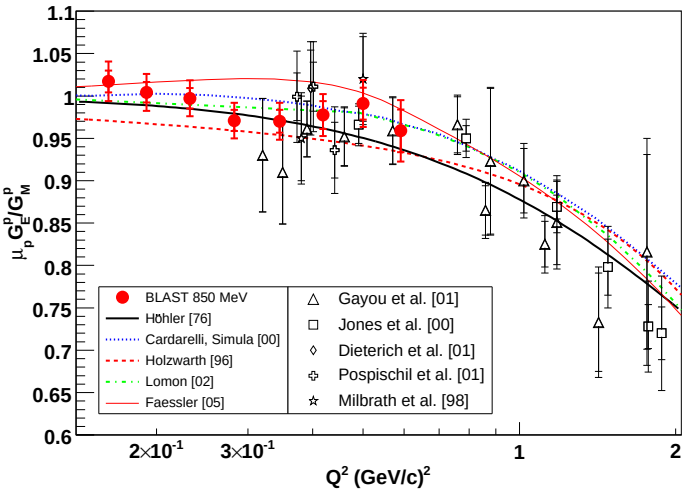

Fig. 2. The BLAST results on the extracted proton electric to magnetic form factor ratio as a function of Q^2 together with world data.

5. Results

Fig. 2 shows the final BLAST results [21] on the extracted proton form factor ratio together with world data from recoil polarization measurements [2,3,4,18,19,20]. The inner error bars are the statistical errors, while the outer errors are the quadrature sum of the statistical and systematic errors. Also shown are a few selected models: the soliton model [31], the extended vector meson dominance model [32], the relativistic constituent quark model (CQM) with SU(6) symmetry breaking, a constituent quark form factor [34], and a Lorentz covariant chiral quark model [35]. In addition, we also show the Höhler [36] parametrization.

In combination with the world cross-section data on *ep* elastic scattering in the same Q^2 values, the proton electric and magnetic form factors have been extracted [21]. Fig. 3 shows the extracted proton electric and magnetic form factors using the BLAST results on the proton form factor ratio, and the precision has been significantly improved compared with results obtained using Rosenbluth separation technique.

Fig. 4 shows the BLAST results [30] on G_E^n extracted from $\vec{d}(\vec{e}, e'n)$ as a function of Q^2. The state-of-the-art calculation by Arenhövel *et al.* [26,37] was used in the Monte Carlo simulation of the BLAST measurement in extracting the G_E^n values. Also shown are the world data on G_E^n from various double polarization measurements [39−46]. The BLAST results are shown with the statistical errors as the inner error bars and outer error bars being the quadrature sum of the statistical and systematic errors. The "BLAST fit" (blue solid line) is a parametrization of the data based on the sum of two dipoles shown with a one-sigma error band. The

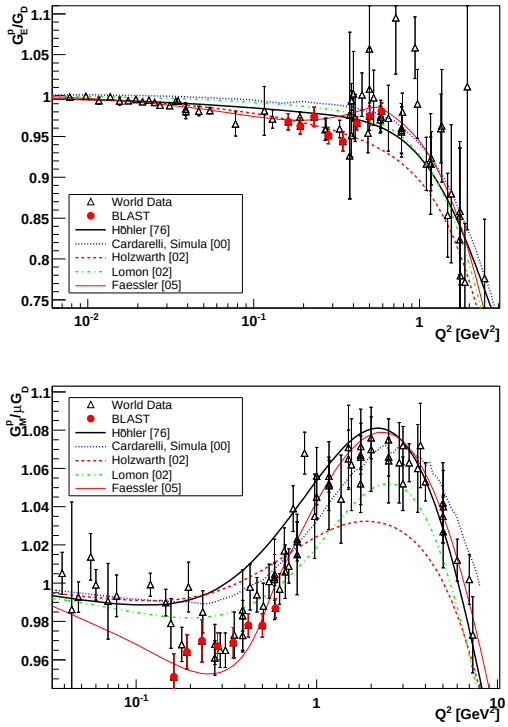

Fig. 3. The BLAST results on the extracted proton electric (upper panel) and magnetic form factor (lower panel) as a function of Q^2 together with world data.

recent parametrization [48] (magenta dash-dotted line) is based on the form introduced by Friedrich and Walcher [47]. Also shown are recent results based on vector meson dominance and dispersion relations (red short-dashed [49,32] and green long-dashed lines [50]), and of a light-front cloudy bag model with relativistic constituent quarks [13] (cyan dotted line).

The new precision data from BLAST have significantly improved our knowledge about the nucleon electromagnetic structure, particularly in the determination of the neutron charge distribution [51]. These new data also present challenges to model calculations of nucleon form factors as well as future more reliable lattice QCD predictions.

6. Acknowledgment

We thank the staff at the MIT-Bates Linear Accelerator Center for the high quality electron beam and for their technical support which made this experiment a success. I thank D. Hasell, X. Qian, R.P. Redwine for careful reading of this paper, and Wei Chen for assistance with Fig. 1. This work is supported by the U.S. Department of

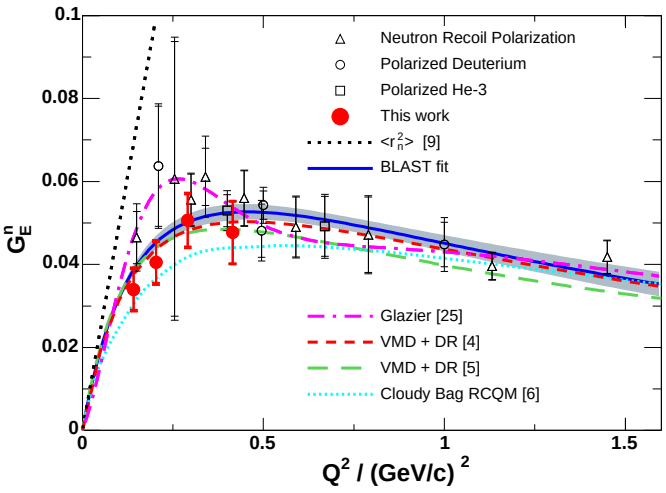

Fig. 4. World data on G_E^n from double-polarization experiments [38]. The data correspond to neutron recoil polarization experiments with unpolarized ^{2}H target (open triangles) and experiments with polarized ^{2}H (open circles; solid red dots = this work [30]) and ^{3}He targets (open squares). The data are shown with statistical (inner error bars) and with statistical and systematic errors added quadratically (outer error bars).

Energy under contract number DE-FC02-94ER40818 and DE-FG02-03ER41231.

References

1. M.N. Rosenbluth, Phys. Rev. **79**, 615 (1950).
2. M. Jones *et al.*, Phys. Rev. Lett. **84**, 1398 (2000).
3. O. Gayou *et al.*, Phys. Rev. C **64**, 038202 (2001); Phys. Rev. Lett. **88**, 092301 (2002).
4. V. Punjabi *et al.*, Phys. Rev. C **71**, 055202 (2005).
5. R.C. Walker *et al.*, Phys. Rev. D. **49**, 5671 (1994).
6. L. Andivahis *et al.*, Phys. Rev. D. **50**, 5491 (1994).
7. M.E. Christy *et al.*, Phys. Rev. C. **70**, 015206 (2004).
8. I.A. Qattan *et al.*, Phys. Rev. Lett. **94**, 142301 (2005).
9. Jefferson Lab Experiment E04-108, Spokerspersons: E. Brash, M. Jones, C. Perdrisat, V. Punjabi.
10. G. P. Lepage and S. J. Brodsky, Phys. Rev. D **22**, 2157 (1980).
11. A.V. Belisky and X.D. Ji and F. Yuan, Phys. Rev. Lett. **91**, 092002 (2003).
12. J. P. Ralston and P. Jain, hep-ph/0207129, (2002); J. P. Ralston, R. V. Buniy and P. Jain, hep-ph/0206063, (2002)
13. G.A. Miller and M.R. Frank, Phys. Rev. C **65**, 065205 (2002).
14. S.J. Brodsky *et al.*, Phys. Rev. D **69**, 076001 (2004).
15. P.A.M. Guichon and M. Vanderhaeghen, Phys. Rev. Lett. **91**, 142303 (2003). P.G. Blunden, W. Melnitchouk, J.A. Tjon, Phys. Rev. Lett. **91**, 142304 (2003); M.P. Rekalo and E. Tomasi-Gustafsson, nucl-th/0307066.
16. Y.C. Chen, A. Afanasev, S.J. Brodsky, C.E. Carlson and M. Vanderhaeghen, Phys.

Rev. Lett. **93**, 122301 (2004); A.V. Afanasev and N.P. Merenkov, Phys. Rev. D **70**, 073002 (2004).
17. Jefferson Lab proposal E04-116, contact person W. Brooks; J. Arrington *et al.*, nucl-ex/0408020; Jefferson Lab experiment E04-019, contact person: R. Suleiman; Jefferson Lab experiment E05-015, contact person: T. Averett; The Olympus proposal at DESY, K. Dow *et al.*, Letter of Intent to DESY PRC, June, 2007.
18. S. Dieterich *et al.*, Phys. Lett. **B500**, 47 (2001).
19. T. Pospischil *et al.*, Eur. Phys. J. **A12**, 125 (2001)
20. B. Milbrath *et al.*, Phys. Rev. Lett. **80**, 452 (1998), Phys. Rev. Lett. **82**, 2221(E) (1999).
21. C. Crawford *et al.*, Phys. Rev. Lett. **98**, 052301 (2007); C. Crawford, Ph.D. thesis, MIT, 2006 (unpublished).
22. H. Gao, Int. J. Mod. Phys. E, **12**, No. 1, 1 (2003).
23. Charles Hyde, Cornelis De Jager, Annu. Rev. Nucl. Part. Sci. **54**, 217 (2004).
24. T.W. Donnelly and A.S. Raskin, Ann. Phys, **169**, 247 (1986).
25. C.B. Crawford, Ph.D. thesis, Massachusetts Institute of Technology (2005).
26. H. Arenhövel, W. Leidemann, and E.L. Tomusiak, Eur. Phys. J. A **23**, 147 (2005); Phys. Rev. C **46**, 455 (1992); H. Arenhövel, W. Leidemann, and E.L. Tomusiak, Z. Phys. A **331**, 123 (1988); Erratum Z. Phys. A **334**, 363 (1989).
27. D. Hasell *et al.*, The BLAST Experiment (to be published).
28. D. Cheever *et al.*, Nucl. Instrum. Methods Phys. Res., Sect. A **556**, 410 (2006); L.D. van Buuren *et al.*, Nucl. Instrum. Methods Phys. Res., Sect. A **474**, 209 (2001).
29. A. Maschinot, Ph.D. thesis, Massachusetts Institute of Technology, 2005; A. DeGrush, Ph.D. thesis, Massachusetts Institute of Technology, in preparation; A. DeGrush *et al.*, to be published.
30. E. Geis *et al.*, Phys. Rev. Lett. **101**, 042501 (2008).
31. G. Holzwarth, Z. Phys. **A356** (1996) 339.
32. E.L. Lomon, Phys. Rev. C **66**, 045501 (2002).
33. G.A. Miller, Phys. Rev. C **66**, 032201(R) (2002).
34. F. Cardarelli and S. Simula, Phys. Rev. **C62** (2000) 065201; S. Simula, e-print nucl-th/0105024; S. Simula, private communication.
35. A. Faessler, Th. Gutsche, V.E. Lyubovitskij, K. Pumsa-ard, Phys. Rev. D **73**, 114021 (2006).
36. G. Höhler *et al.*, *Nucl. Phys.* **B114**, 505 (1976).
37. H. Arenhövel, private communications.
38. B. Plaster *et al.*, Phys. Rev. C **73**, 025205 (2006) and references therein.
39. H. Zhu *et al.*, Phys. Rev. Lett. **87**, 081801 (2001).
40. G. Warren *et al.*, Phys. Rev. Lett. **92**, 042301 (2004).
41. I. Passchier *et al.*, Phys. Rev. Lett. **82**, 4988 (1999).
42. T. Eden *et al.*, Phys. Rev. C **50**, R1749 (1994).
43. M. Ostrick *et al.*, Phys. Rev. Lett. **83**, 276 (1999).
44. C. Herberg *et al.*, Eur. Phys. J. A **5**, 131 (1999).
45. J. Becker *et al.*, Eur. Phys. Jour. A **6**, 329 (1999).
46. D. Rohe *et al.*, Phys. Rev. Lett. **83**, 4257 (1999).
47. J. Friedrich and Th. Walcher, Eur. Phys. J. A **17**, 607 (2003).
48. D.I. Glazier *et al.*, Eur. Phys. J. A **24**, 101 (2005).
49. E.L. Lomon, arXiv:nucl-th/0609020v2; to be published and private communication.
50. M.A. Belushkin, H.-W. Hammer, and Ulf-G. Meißner, Phys. Rev. C **75**, 035202 (2007).
51. C. Crawford *et al.*, to be published.